A host-adapted commensal fungus from pet store mice drives type 2 immunity and cross-kingdom protection

Geongoo Han[1], Rebecca Yunker[1], Mohammad H. Hasan[1], Alex Bruce[1], Kellie Baldaro[1], Jessica Pacia[1], Nicholas N. Jarjour[2,3], Lalit K. Beura[1,*], Shipra Vaishnava[1,*]

[1] Molecular Microbiology & Immunology Department, Brown University, Providence, RI 02912, USA.

[2] Center for Immunology, University of Minnesota, Minneapolis, MN 55455, USA.

[3] Department of Laboratory Medicine and Pathology, University of Minnesota, Minneapolis, MN 55455, USA.

* Corresponding author: lalit_beura@brown.edu, shipra_vaishnava@brown.edu

Abstract

Naturalized, wilded, wildling, and dirty/pet store mouse models represent a spectrum of approaches designed to make laboratory mice more immunologically and physiologically similar to wild or human contexts by increasing their exposure to naturally occurring microbes and pathogens. In this study, we screened the gut mycobiome of pet store mice, and identified *Kazachstania pintolopesii* as a dominant fungus in pet store mice across various geographical locations. *K. pintolopesii* strains isolated from mice in geographically distinct pet stores stably colonize the gastrointestinal tract of laboratory mice, independent of gut bacterial composition, maintaining high fungal burdens for extended periods. *K. pintolopesii* rapidly became the dominant fungus in the mouse gut in conventional, antibiotic, and germ-free settings, outcompeting other non-murine fungal strains. Pet store-derived *K. pintolopesii* exhibited unique immunological properties distinct from typical anti-fungal responses. Unlike *C. albicans* colonization, *K. pintolopesii* did not induce circulating neutrophil expansion or Th17 cell populations in the gut mucosa. When administered systemically, *K. pintolopesii*-infected mice showed 100% survival with minimal fungal burden in kidneys, contrasting sharply with lethal *C. albicans* infections. Adaptive immune deficiency (Rag1 knockout mice) did not affect *K. pintolopesii* colonization or host response, indicating that B and T cell-mediated immunity does not restrain this fungus. *K. pintolopesii* colonization provided no cross-protection against systemic candidiasis further establishing lack of immune activation. These findings demonstrate that *K. pintolopesii* establishes a benign host-fungal relationship through neutrophil-independent mechanisms, avoiding classical anti-fungal immune activation while maintaining stable gut colonization. Instead, it selectively induces strong type 2

mucosal immune responses, increasing tuft and goblet cell counts and stimulating Th2 and group 2 innate lymphoid cell (ILC2) populations. This immune profile confers notable protection against intestinal nematode infection, demonstrated by reduced *Heligmosomoides polygyrus* egg counts. Altogether, *K. pintolopesii* serves as an exemplary model for commensal mycobiota, revealing distinct mechanisms for host tolerance and immune modulation.

Keywords

Kazachstania pintolopesii, commensal fungi, host adaptation, microbiome, cross-kingdom protection, type 2 immunity

Introduction

Commensal microorganisms are crucial for host immunity and have coevolved with their natural hosts, often exhibiting high species restriction. This phenomenon is observed across various life forms. In invertebrates, the Hawaiian bobtail squid depends on *Vibrio fischeri* for tissue development [1], while tsetse flies rely on *Wigglesworthia glossinidia* for fitness and reproduction [2]. Similarly, in mammals, gut immune cell maturation is driven by host-specific bacteria. Experiments have shown that human or rat gut bacteria introduced into germ-free (GF) mice are less effective at stimulating immune cell development compared to mouse-specific bacteria, highlighting the importance of host-adapted microbes in shaping host physiology [3]. The mammalian gut houses a complex ecosystem of microbes, including bacteria, viruses, and fungi. However, our understanding of whether and how commensal fungi interact exclusively with their hosts is limited due to the lack of true commensal models that can stably colonize the mouse gut without causing inflammation or requiring immune suppression. Most research efforts have focused on *Candida albicans,* a gut commensal that is the main cause of opportunistic infections in humans. However, studying *C. albicans* commensalism in humans is somewhat limited because of technical and ethical challenges. As such introducing *C. albicans* to the murine gut has emerged as a dominant model system. But this approach often requires antibiotic treatment to maintain stable colonization and can induce inflammatory responses compromising interpretation [4-6]. Therefore, alternative commensal fungi that have coevolved with their natural host are needed to better understand fungal-host symbiosis.

In recent years, researchers have embraced alternative models of microbial exposure for laboratory mice to better simulate the complex immune challenges faced by wild

mammals. Approaches such as "re-wilded" models—where laboratory mice are released into natural environments[7] or “wildling models” where embryos of laboratory mice are transferred into wild-caught female mice[8]—have been developed to introduce a broader range of natural microbiota and pathogens during early life. Another widely used strategy is the creation of "dirty mice," which involves co-housing standard laboratory mice with pet store or wild-derived mice, thereby facilitating the transmission of diverse microbes between animals and mimicking the microbial exposures found in free-living populations[9-11]. Studies using these models have demonstrated that increased microbial exposure leads to the development of an "immunologically experienced" immune system, marked by higher levels of memory T cells, diverse subsets of specialized immune cells, and enhanced inflammatory responses. The differences in microbial exposure between laboratory, wild, and pet store mice present a unique opportunity to identify and characterize potential commensal fungi that have co-evolved with their murine hosts [7,12].

Previous studies have used re-wilded mouse models to study naturally occurring fungi and found that fungal colonization in re-wilded mice led to sustained neutrophil expansion and protected against bloodborne bacterial infection with *Staphylococcus aureus*[7]. In a comparative study of wildlings, wild mice, and conventional laboratory mice, wildlings and wild mice exhibited a much higher proportion of fungal DNA compared to the total DNA present than their conventional lab counterparts[8]. Furthermore, the composition of fungal communities differed: wildlings and wild mice had markedly more *Ascomycota* and much less *Basidiomycota* than conventional laboratory mice. In this study, we sought to isolate and characterize commensal fungi from pet store mice to elucidate their unique interactions with the host. Pet store mice carry a diverse and complex microbial

community, including microbes and pathogens similar to those found in more natural, less sanitized environments. Laboratory mice cohoused with pet store mice become "dirty" mice, experiencing a natural-like microbial environment that results in mature and more human-like immune responses[9]. These features enable novel research opportunities to identify previously unrecognized host-microbe and microbe-microbe interactions. The multitude of microbiota transmitted—including viruses, bacteria, fungi, and eukaryotic organisms—facilitates the study of microbial succession, competition, synergy, and cross-kingdom interactions within the host, with observable impacts on immune cell phenotypes, cytokine production, and pathogen resistance. By scoping the gut microbiome of pet store mice from geographically distinct regions, we identified *Kazachstania pintolopesii* as the dominant fungal species. *Kazachastania* spp, were recently also characterized from laboratory as well as wild-caught mice[13,14]. Through a series of *in vivo* experiments and multi-omics analyses, we investigated the colonization dynamics and host immune responses upon the pet store *K. pintolopesii* strain colonization in conventional, antibiotics-treated, GF, and gnotobiotic laboratory mice. Like the previous studies, we found that *K. pintolopessii* strains isolated from pet store mice had superior ability to colonize laboratory mice irrespective of commensal bacteria rapidly outcompeting non-native fungal species. Additionally, we established that pet store-derived *K. pintolopesii* displays a benign immunological signature, distinct from *Candida albicans*, a human fungal commensal. This discovery marks the fungal commensalism, opening avenues for exploring how such interactions influence immune responses and microbial competition and sets a benchmark for commensal mycobiota.

118 **Results**

119 ***K. pintolopesii* is the dominant gut fungus in pet store mice**

120 SPF laboratory mice are maintained in controlled environments, shielded from potential
121 pathogen exposure, and typically harbor microorganisms with limited diversity. In contrast,
122 pet store mice live in large breeding colonies and are routinely exposed to rich varieties
123 of microbes, including pathogenic bacteria, viruses, parasites, and fungi [9]. As an example
124 of this, electron microscopic imaging of the gut epithelial surface of laboratory mice
125 revealed no significant epithelium-attached microbes. In contrast, the epithelial surfaces
126 of pet store mice harbored many microbial-like structures of varying shapes and sizes
127 (~2-15 μm) (Fig. 1A). Therefore, we used pet store mice as a source to screen for
128 commensal murine fungi.

129 Using ribosomal RNA-based probes, we were able to find presence of fungal species
130 among these epithelial-associated microbes in pet store mice, which are largely absent
131 in laboratory mice (Fig.1B). Fungal burden in the feces of pet store mice was notably high
132 (~10^7 CFU/g of feces), while no fungal populations were detectable in the feces of
133 laboratory mice in our facility (Fig. 1C). Fungal colonization was observed throughout the
134 gastrointestinal tract of the pet store mice, from the duodenum to the feces, with the fungal
135 burden progressively increasing toward the caudal end of the intestine indicating that pet
136 store mice are heavily colonized with fungi throughout the gastrointestinal tract (Fig. 1D).

137 To identify the commensal fungal species in the murine gut, we cultured the gut
138 contents of the pet store mice for 5 days at 30 °C and randomly picked 26 colonies from
139 the plates. Sequencing of the internal transcribed spacer (ITS) region of these colonies
140 revealed that all colonies are the same fungal species, *Kazachstania pintolopesii* (Fig.

141 S1A). The isolate appeared as a budding yeast and had an ellipsoidal shape with typical
142 yeast cell structures such as a thick cell wall, nucleus, vacuole, and mitochondria (Fig.
143 S1B and C). The isolate showed higher ITS sequence similarities with other *Kazachstania*
144 species and *Saccharomyces cerevisiae*, whereas lower similarities with *Candida* and
145 *Aspergillus* species (Fig. S1D). We also directly sequenced the ITS1 region of the gut
146 metagenome of pet store mice. Intriguingly, this culture-independent analysis also
147 showed that the intestines of pet store mice were predominantly colonized by a single
148 fungal species, *K. pintolopesii*, which accounted for over 99% of the total sequence reads
149 in both the luminal and mucosal regions of the small intestine and colon (Fig. 1E).

150 To determine whether this observation is specific to pet stores in a particular region
151 (Rhode Island), fecal samples were collected from pet store mice in other geographical
152 locations, including the Midwest United States (Minnesota) and the Southern United
153 States (Texas) (Fig. S1E). Higher fungal burden was observed across all regions (Fig.
154 1F), with *K. pintolopesii* consistently identified as the predominant fungal species in the
155 gut, regardless of the region (Fig. 1G). These findings indicate that *K. pintolopesii* is not
156 limited to a specific geographical area but rather is a prevalent member of the mouse
157 mycobiome under non-laboratory settings. It colonizes the gastrointestinal tract
158 extensively, achieving high population levels both near the mucosal surface and within
159 the intestinal lumen.

160 ***K. pintolopesii* stably colonizes laboratory mice irrespective of gut bacteria and**
161 **provides colonization resistance against non-murine fungi**

162 To test whether this fungal isolate from the pet store mice could colonize the intestines of
163 the laboratory mice, we orally administered the isolated *K. pintolopesii* to laboratory mice.

164 The isolated fungus colonized throughout the gastrointestinal tract, from the esophagus
165 to the feces, of the laboratory mice (Fig. 2A). Furthermore, a high fungal burden (~10^7
166 CFU/g in the feces) was maintained for at least 6 weeks (Fig. S2A). The colonized *K.*
167 *pintolopesii* was located closely to the gut epithelium of mice, co-localizing with bacteria,
168 similar to the fungal colonization pattern observed in the pet store mice (Fig. S2B).

169 The laboratory mice from various vendors have different bacterial communities in the
170 gut [15,16]. To test the colonization of *K. pintolopesii* in different bacterial compositions, we
171 colonized the fungal isolate in mice bred at Brown University (Brown), Jackson Laboratory
172 (Jax), and Taconic Biosciences (Tac). A high burden of *K. pintolopesii* (~10^7 CFU/g) was
173 observed in the feces of Brown, Jax, and Tac mice (Fig. S2C). GF mice showed a
174 comparable level of *K. pintolopesii* fecal colonization to other laboratory mice (Fig. S2D),
175 demonstrating that the presence of commensal bacteria does not influence *K.*
176 *pintolopesii*'s intestinal colonization. We performed 16S rRNA gene sequencing to assess
177 the impact of *K. pintolopesii* colonization on the gut bacterial community, and *K.*
178 *pintolopesii* colonization maintained bacterial community diversity, composition, and load
179 without significant alterations (Fig. S2E-H). The ability of *K. pintolopesii* to colonize the
180 gastrointestinal tract to high levels without impacting the bacterial community is in contrast
181 to other fungal species that often require microbiome manipulation to establish
182 colonization [4,5,17-19].

183 Recent studies showed that murine *Kazachstania* strains inhibited the other fungal
184 growth in the mouse intestines [13,14]. To examine whether the *K. pintolopesii* isolate affects
185 the colonization of non-murine-specific fungi, a competition assay was conducted. The
186 assay included five fungal species: *K. pintolopesii* and four other fungal species - *S.*

187 *cerevisiae* BY4717*, C. albicans* SC5314*, C. parapsilosis* ATCC22019, and *C. tropicalis*
188 MYA-3404 [18-22] (Fig. S3A). An equal number of viable fungal cells (~2 × 10^6 CFU/species)
189 were orally administered simultaneously to both conventional mice and GF mice, and
190 fecal samples were collected, followed by ITS sequencing. Notably, *K. pintolopesii*
191 exhibited outstanding colonization ability, out-competing the other fungal species in both
192 conventional and GF mice (Fig. S3B and C). In conventional mice, *K. pintolopesii* rapidly
193 dominated the fungal community, accounting for over 95% of the total fungal population
194 within 3 days of treatment (Fig. S3B). In GF mice, *C. albicans* SC5314 was initially the
195 dominant species, with *C. tropicalis* MYA-3404 comprising over 10% of the population
196 until day 7. However, the proportion of *K. pintolopesii* increased over time, eventually
197 representing approximately 75% of the total fungal population by days 14 and 22 (Fig.
198 S3C).

199 *C. albicans* SC5314 strain, the standard laboratory isolate, was used for the
200 competition assay, but this strain is not murine-colonizing in the presence of commensal
201 bacteria. In contrast, *C. albicans* 529L is a clinical isolate from the oral cavity and
202 colonizes the murine gut without antibiotic treatment [23,24]. We conducted another
203 competition assay with *C. albicans* 529L to test whether *K. pintolopesii* can outcompete
204 other fungal species in the presence of a murine-colonizing strain (Fig. 2B). In the
205 absence of *K. pintolopesii*, *C. albicans* 529L was the most abundant fungal species and
206 stably colonized in conventional mice (Fig. 2C and E). However, the addition of *K.*
207 *pintolopesii* lowered the *C. albicans* 529L burden and outcompeted other fungal members
208 (Fig. 2C, D, and F). In antibiotic-treated mice, the burden of *C. albicans* 529L was lower

209 in the presence of *K. pintolopesii,* and the proportion of *K. pintolopesii* DNA was the most
210 abundant among the fungal members at day 14 (Fig. S3D–G).
211 This suggests that *K. pintolopesii* is capable of stable colonization in laboratory mice,
212 independent of the presence of commensal gut bacteria, and provides colonization
213 resistance against non-murine fungi.

214 ***K. pintolopesii* colonization does not induce classical anti-fungal immune**
215 **responses, including expansion of neutrophils and the Th17 population**

216 Fungal colonization in the gut has been reported to trigger immune responses, including
217 the expansion of neutrophils and T helper 17 cells (Th17) populations. *C. albicans*, a well-
218 studied human commensal fungus, is known to induce neutrophils and Th17 populations
219 in humans and mice [25,26]. Rewilded mice, which harbor an increased fungal population in
220 the gut, exhibited increased circulating neutrophil levels [7,12]. In addition, mucosa-
221 associated fungi induced type 17 immune responses [27]. Interestingly, it was reported that
222 intestinal colonization of *Kazachstania heterogenica* var. *weizmannii,* another murine-
223 derived *Kazachstania* species, does not induce systemic neutrophilia and Th17
224 populations in lymph nodes, unlike *C. albicans* [13]. To evaluate whether *K. pintolopesii*
225 also induces the aforementioned classical anti-fungal immune responses, we measured
226 the levels of neutrophils in blood upon the *K. pintolopesii* colonization. Interestingly, *K.*
227 *pintolopesii* colonization did not induce circulating neutrophil levels in the peripheral blood
228 (Fig. 3A). To mimic the systemic fungal dissemination, we introduced *K. pintolopesii*
229 intravenously in mice, comparing it with *C. albicans* systemic infection (Fig. 3B). As
230 expected, *C. albicans*-infected mice exhibited a poor survival rate and a high fungal
231 burden in the kidneys, along with significant upregulation of *Il17a* gene expression in the

232 kidney. Intriguingly, *K. pintolopesii*-infected mice did not show any pathological symptoms.
233 All *K. pintolopesii*-infected mice survived and showed low to no detectable levels of fungal
234 burden in the kidney. Additionally, *Il17a* gene expression in the kidney of *K. pintolopesii*-
235 infected mice was significantly lower, approximately 14-fold lower than that observed in
236 *C. albicans*-infected mice. (Fig. 3C – E). To assess neutrophils' role in *K. pintolopesii*
237 clearance during systemic infection, we depleted neutrophils using anti-Ly-6G (1A8 clone)
238 antibody before *K. pintolopesii* infection (Fig. 3F). Despite complete neutrophil depletion,
239 all mice survived without detectable kidney fungal burden (Fig. 3G-H and S4).

240 To assess the contribution of the adaptive immune system in colonization of
241 commensal fungi, we introduced *K. pintolopesii* to Rag1 knock-out (KO) mice (Fig. 4A).
242 Neither the body weight nor the fungal burden differed between wild-type (WT) and Rag1
243 KO mice (Fig. 4B and C). To assess the potential for systemic fungal dissemination and
244 immune activation in the absence of B and T lymphocytes, we measured the number of
245 neutrophils in the spleen. No significant differences were observed in neutrophil density
246 between the two genotypes, indicating that the adaptive immune arms are neither
247 engaged nor play a significant role in limiting *K. pintolopesii* burden (Fig. 4D). We also
248 measured the levels of Th17, another key anti-fungal immune cell in mucosal immunity,
249 following *K. pintolopesii* colonization. Interestingly, *K. pintolopesii* colonization did not
250 increase Th17 cells in the small intestinal lamina propria (Fig. 4E).

251 The intestinal *C. albicans* colonization protects the host against systemic *C. albicans*
252 infection [26]. To assess whether the commensal fungus provides a similar cross-species
253 protection to the host, *C. albicans* was systemically introduced into *K. pintolopesii*-
254 colonized mice (Fig. 5A). However, no differences in survival rates or fungal burden in the

255 kidneys were observed between the control and *K. pintolopesii*-colonized mice following
256 systemic *C. albicans* infection (Fig. 5B and C). In contrast, we observed that the intestinal
257 colonization by *C. albicans* in antibiotics-treated mice protected the host from systemic
258 candidiasis (Fig. 5D – F).

259 These results indicate that *K. pintolopesii* does not trigger classical anti-fungal defenses,
260 including neutrophilia and Th17 response, which have been previously reported in
261 response to other *Kazachstania* strains [13,14]. And the complete absence of the adaptive
262 arm of the immune system does not enhance fungal pathogenicity. When *K. pintolopesii*
263 was introduced systemically, the host was able to control the fungus via neutrophil-
264 independent mechanisms, suggesting a unique host-fungal relationship that differs from
265 typical anti-fungal immune responses.

266 ***K. pintolopesii* colonization induces type 2 immune responses in the gut and**
267 **protects the host against roundworm infection**

268 Although we examined the effects of *K. pintolopesii* colonization on the host immune
269 system, we primarily focused on dominant anti-fungal immune responses, specifically
270 neutrophils and Th17 cells. However, to thoroughly investigate the impact of *K.*
271 *pintolopesii* colonization on the host's intestine in an unbiased manner, we collected ileum
272 samples 14 days post-colonization and performed bulk RNA sequencing. *K. pintolopesii*
273 colonization showed significant transcriptional changes with 602 up-regulated genes and
274 1,213 down-regulated genes compared with control mice (Fig. S5). Notably, tuft cell and
275 goblet cell marker genes were remarkably upregulated following *K. pintolopesii*
276 colonization (Fig. 6A). To validate the RNA sequencing data, we quantified the number
277 of tuft cells and goblet cells in the small intestine. As we saw in RNA sequencing data,

278 the number of tuft cells and goblet cells was significantly higher in *K. pintolopesii*-
279 colonized mice than in control mice (Fig. 6B and C). Tuft cells are a rare cell type in the
280 intestinal epithelium, yet they play a pivotal role in goblet cell hyperplasia and in initiating
281 type 2 immune responses [28,29]. So, next examined *K. pintolopesii* also modulates other
282 type 2-associated cells. We observed significant upregulation of T helper 2 (Th2) and
283 group 2 innate lymphoid cells (ILC2s) by *K. pintolopesii* colonization (Fig. 6D and S6A).
284 To check if this induction of type-2 immunity is not limited only to the C57BL/6 mouse
285 strain, we colonized *K. pintolopesii* in the prototypical Th2-type mice, BALB/c [30,31].
286 Colonized BALB/c mice exhibited a high fungal burden (Fig. 6E) and significantly
287 increased frequencies of Th2 and ILC2 levels in the small intestine, similar to what was
288 observed in C57BL/6 mice (Fig. 6F and S6B). However, circulating neutrophil levels and
289 the Th17 population in the small intestine were comparable to those in control mice (Fig.
290 S6C and D).
291 Next, to assess the functional relevance of this type-2 immunity, we challenged control
292 and *K. pintolopesii*-colonized mice with a murine intestinal nematode, *Heligmosomoides*
293 *polygyrus*, that is controlled by type-2 immune responses (Fig. 6G). The number of eggs
294 in the fecal samples was significantly lower in *K. pintolopesii*-colonized mice compared
295 with control mice at 21 days post-infection (Fig. 6H). This suggests that *K. pintolopesii*
296 colonization in the mouse intestine protects the host from a parasitic nematode.
297
298

Discussion

Naturalized, wilded, and pet store-cohoused mice have emerged as valuable models for studying the impact of microbes encountered outside the laboratory setting. These mice provide researchers with a more accurate representation of the complex microbial interactions that occur in natural environments, offering insights that conventional laboratory mice cannot. Transfer of gut microbiome from wild mice to the GF mice exhibited improved protection against viral infection, and embryo transfer of laboratory mice into wild mice showed human-like immune phenotypes [8,32]. Exposing laboratory mice to wild environments and then recapturing them is another way to colonize the wild microbiome in laboratory mice. These rewilded mice exhibit increased circulating neutrophils and enhanced granulopoiesis [7,12]. Pet store mice are another valuable resource for studying host-microbe interactions in mice. Although they do not live in the natural environment like wild mice, they are exposed to the dirty environment in which humans live. When laboratory mice are exposed to the pet store mice microbiome by co-housing, co-housed laboratory mice harbor various microbes, such as viruses, fungi, and worms, and exhibit a similar immune composition to that of human adults [9,33].

While studies have explored interactions between mice and their complex microbiomes in toto, the specific relationships between hosts and individual microbial kingdoms are less explored, especially in the presence of diverse pathogenic groups. Among various microbes, we focused on the role of commensal fungi in the murine gut. Fungi ubiquitously exist in various environments, including multiple body sites of mammals [34]. In general, the importance of commensal fungi is underestimated compared to commensal bacteria due to fewer available databases and lower cell numbers compared to bacteria in the gut.

322 However, fungi can contribute unique metabolic functions as eukaryotes, and even a
323 minor commensal member can affect host phenotypes in the gut [15,35,36]. In our study, we
324 aimed to identify murine commensal fungi that will allow us to take advantage of the robust
325 mouse model to study fungal commensalism. We successfully isolated *K. pintolopesii*
326 from the intestines of pet store mice, which constituted the dominant fungal species in the
327 pet store mice regardless of geographic location. In laboratory settings, *K. pintolopesii*
328 was capable of stable colonization without any manipulation of the gut microbiome and
329 was not harmful to the host.

330 Two recent studies also identified *Kazachstania* species from immunodeficient and wild
331 mice that can colonize the gut of laboratory mice to high numbers. While the study by
332 Kralova et al. investigates *Kazachstania heterogenica* var. *weizmannii* isolated from an
333 immunodeficient mouse model [13], the study by Liao et al. examines *K. pintolopesii*
334 isolated from free-living mice [14]. The *Kazachastania* sp. in all three studies demonstrates
335 a remarkable ability to colonize the murine gastrointestinal tract and outcompete or
336 prevent colonization by non-murine fungi, including *C. albicans*, showcasing their
337 potential as powerful modulators of the gut mycobiome. Other studies using the wildling
338 mice also support that *K. pintolopesii* is a dominant commensal fungus of the mouse
339 intestine [37,38].

340 *K. weizmannii* exhibits a stealth colonization strategy, inducing minimal immune
341 responses under normal conditions but mitigating *C. albicans*-induced pathology [13]. In
342 contrast, *K. pintolopesii* isolated in Liao et al. and our study triggers a robust type 2
343 immune response, enhancing resistance to helminth infections while exacerbating
344 gastrointestinal allergy [14].

The Liao et al. study shows that *K. pintolopesii* triggers a type 2 immune response, characterized by eosinophilia and Th2 cell polarization, but only when the mucosal barrier is impaired (e.g., during fiber-free diet, antibiotic treatment, or in GF mice) [14]. In contrast, we observed that the *K. pintolopesii* strain from pet store mice increases type 2 immune cells in the small intestine and provides cross-kingdom protection against helminth infection even without any need for barrier impairment, suggesting strain-level differences in *K. pintolopesii* mice strains between the two studies. Perhaps the microbial environment of pet store mice, which have a higher burden of parasitic worms and pathogens, has forced *K. pintolopesii* to induce type 2 immunity [39-41]. Cross-kingdom interactions highlight the complexity and interconnectedness of microbial communities and their host organisms. These interactions can have significant implications for understanding disease resistance, developing new therapeutic strategies, and managing ecosystems.

In conclusion, our study underscores the critical importance of strain-specific, commensal fungal interactions in shaping the gut mycobiome and influencing host physiology. Future strain-level studies of commensal fungi will provide deeper insights into host-fungal commensalism. The discovery of the current study will lead to a more nuanced understanding of how commensal fungi contribute to host health, influence immune system development, and potentially protect against pathogens or modulate disease outcomes. This approach could reveal new therapeutic targets or probiotic strategies for improving gut health and managing various gastrointestinal disorders.

367 **Methods**

368 **Mice**

369 Conventional wild-type C57BL/6 mice were purchased from Jackson Laboratory and
370 Taconic Biosciences or were bred in the animal facility at Brown University. BALB/c mice
371 were purchased from Jackson Laboratory. Rag1 KO mice were used as an adaptive
372 immunity-deficient mouse model. GF mice were wild-type C57BL/6 background, and they
373 were raised and bred in flexible film isolators in a gnotobiotic facility at Brown University.
374 Pet store mice were purchased from local pet stores. Fecal pellets of pet store mice in
375 Minnesota and Texas were freshly delivered to Brown University and used for further
376 experiments. Experiments were performed according to the protocols approved by the
377 Institutional Animal Care and Use Committees of Brown University.

378 **Fungal isolation from the gut of pet store mice**

379 Cecal contents and feces, collected from pet store mice, were suspended in sterile PBS
380 and plated on Sabouraud Dextrose (SD) agar with streptomycin (40 mg/L), followed by
381 incubation at 30 °C for 5 days. A total of 26 single colonies were randomly picked from
382 the plates, and the ITS region of fungal colonies was amplified by colony PCR using the
383 Phire Green Hot Start II PCR Master Mix (Thermo Scientific) with ITS1-F/ITS4 primer pair
384 (ITS1-F: 5'-CTTGGTCATTTAGAGGAAGTAA-3', ITS4: 5'-
385 TCCTCCGCTTATTGATATGC-3') [42,43]. The amplification program consisted of 94 °C for
386 10 min, followed by 35 cycles of 94 °C for 30 sec, 52 °C for 30 sec, and 72 °C for 1 min,
387 and 72 °C for 8 min. The amplicon was sequenced by Sanger sequencing (GENEWIZ),
388 and MOLE-BLAST (Basic Local Alignment Search Tool) was performed against the ITS

389 database of NCBI to identify the isolated colonies. The exported phylogenetic tree from
390 MOLE-BLAST was visualized using the R package *ggtree*.

391 **Fungal culture**

392 All fungal strains were cultured in SD or yeast extract-peptone-dextrose (YPD) media.
393 The isolate, *K. pintolopesii*, was cultured at 37 °C for 1 day with shaking. This culture was
394 inoculated in fresh media and cultured for 1 day under the same conditions. *S. cerevisiae*
395 BY4717 was cultured at 30 °C for 2 days with shaking. *C. albicans* SC5314, *C. albicans*
396 529L, *C. parapsilosis* ATCC22019, and *C. tropicalis* MYA-3404 were cultured overnight
397 at 30 °C with shaking. For systemic infection, the *C. albicans* overnight culture was
398 inoculated in fresh media and cultured for 4 h under the same conditions.

399 **Fungal infection**

400 For intestinal colonization of non-colonizing fungi, antibiotic water was prepared with
401 penicillin (750 U/mL), streptomycin (1 mg/mL), and 2.5% (w/v) glucose. *C. albicans*
402 cultures (~10^6 CFU/mL) were resuspended in antibiotic water and administered. The
403 same antibiotic water was provided to mice in both the control and *K. pintolopesii* groups.
404 All antibiotic waters were administered starting four days prior to oral inoculation. One
405 day later, the fungal antibiotic water was replaced with fresh antibiotic water, and fresh
406 antibiotic water was provided every three or four days throughout the whole experimental
407 period. For systemic infections, *K. pintolopesii* (~10^5 CFU/200 μL) or *C. albicans* (~10^5
408 CFU/200 μL) was injected into mice via the retro-orbital venous sinus or lateral tail vein.

409 All fungal cultures were washed twice with sterile PBS and resuspended in the proper
410 solution for infection.

411 The fecal pellets and the contents of the intestine were resuspended in sterile PBS with
412 antibiotics (500 mg/L ampicillin, 250 mg/L streptomycin, 225 mg/L kanamycin) to
413 determine fungal burden. The other tissues were homogenized in sterile PBS with
414 antibiotics. All samples were serially diluted in sterile PBS with antibiotics and plated on
415 SD agar with streptomycin (40 mg/L), followed by incubation at 30 °C or 37 °C for 1 or 2
416 days based on the optimal condition of each fungus.

417 **Fungal competition assay**

418 For oral administration of various fungal species, each fungal culture was mixed with the
419 same CFU and gavaged to conventional, antibiotics-treated mice, or GF mice (~2×10^6
420 CFU/species in 200 μL per mouse).

421 N-acetyl transferase (NAT)-integrated *C. albicans* 529L strain was used for the
422 treatment. To determine *C. albicans* 529L burden, fecal samples were plated on YPD
423 agar plates with streptomycin (40 mg/L) and nourseothricin sulfate (200 mg/L), followed
424 by incubation at 30 °C for 1 day. Fecal *K. pintolopesii* burden was determined by the
425 colony morphology on SD agar plates with streptomycin (40 mg/L), followed by incubation
426 at 37 °C for 2 days.

427 **Immune cell isolation and flow cytometry**

428 To isolate peripheral blood lymphocytes, blood samples were collected from the
429 submandibular vein by cheek punch in heparin-containing polypropylene tubes. Red
430 blood cells were removed from blood samples by two rounds of ACK (Ammonium-
431 Chloride-Potassium) lysis buffer treatment. Lymphocytes from the spleen and the small
432 intestinal lamina propria were isolated as described in Beura et al. [44] and Grizotte-Lake
433 et al. [45].

434 Isolated cells were stained with the corresponding cocktail of fluorescently labeled
435 antibodies (CD3, CD4, CD8a, CD11b, CD45, CD90.2, B220, Ly6C, Ly6G, ST2) and
436 biotin-conjugated anti-mouse lineage (CD3ε, CD11b, CD19, Ly6G/Ly6C) and streptavidin.
437 Cell viability was determined using Ghost Dye 780 or Fixable Viability Dye eFluor™ 450.
438 After surface staining, cells were fixed and permeabilized, followed by intracellular
439 staining with the corresponding cocktail of fluorescently labeled antibodies (Foxp3,
440 GATA3, RORγT, IL-17A). The stained samples were acquired using the Aurora flow
441 cytometer (Cytek) and were analyzed with FlowJo 10 software (BD).

442 **Neutrophil depletion**

443 For neutrophil depletion, anti-Ly-6G antibody (1A8 clone; Biolegend) or isotype control
444 (Biolegend) was administered intraperitoneally to mice every other day (200 μg in 200 μL
445 per mouse) from the day before the *K. pintolopesii* challenge.

446 **DNA extraction for microbiome and mycobiome analysis**

447 The small intestine (ileum) and colon were flushed with sterile PBS to collect luminal
448 contents, and intestinal material was obtained by centrifugation at 5,000 rpm for 10 min.
449 After the flush, the small intestine and colon were scraped and collected in sterile PBS,
450 followed by centrifugation at 5,000 rpm for 10 min to get mucosal contents. Fecal samples
451 were directly collected from the rectum. Samples (~50 mg) were suspended in 50 mM
452 Tris buffer (pH 7.5) supplemented with 1 mM EDTA, 0.2% β-mercaptoethanol, and 1000
453 units/mL of lyticase (Sigma-Aldrich), followed by incubation at 37 °C for 30 min. After
454 incubation, genomic DNA was extracted from samples using a Quick-DNA Fecal/Soil
455 Microbe Microprep Kit (Zymo Research) according to the manufacturer's protocol and
456 was stored at −20°C until further processing.

457 **Bacterial load measurement**

458 Bacterial load in the feces was measured by quantitative real-time PCR (qPCR).
459 Reactions were prepared using Maxima SYBR Green/ROX qPCR Master Mix (Thermo
460 Scientific). Bacterial DNA contents in the intestine were determined by 16S rRNA gene
461 contents using the 340F/514R primer pair (340F: 5'-ACTCCTACGGGAGGCAGCAGT-3',
462 514R: 5'-ATTACCGCGGCTGCTGGC-3'). Bacterial load was expressed as a 2^{-Ct} value
463 and normalized to the weight of the starting fecal material.

464 **16S rRNA gene sequencing and bacterial community analysis**

465 The V4/V5 region of the bacterial 16S rRNA gene was amplified using the Phusion High-
466 Fidelity DNA polymerase (Thermo Scientific) with 518F/926R primer pair (518F: 5'-
467 CCAGCAGCYGCGGTAAN -3', 926R: 5'- CCGTCAATTCNTTTRAGT -3'), which were
468 conjugated with overhang adapter sequences for Illumina MiSeq. The amplification
469 program consisted of 95 °C for 3 min, followed by 35 cycles of 95 °C for 30 sec, 58 °C for
470 30 sec, and 72 °C for 30 sec, and 72 °C for 10 min. DNA libraries were constructed and
471 sequenced on Illumina MiSeq 2 × 300 bp paired-end sequencing (Rhode Island
472 Genomics and Sequencing Center).

473 The raw sequencing reads were processed using the QIIME2 pipeline [46]. DADA2 [47]
474 was used to perform denoising and to construct the amplicon sequence variants (ASVs)
475 table. The pre-trained Naïve Bayes classifier on the SILVA 132 database [48] was used for
476 taxonomic assignment. Singletons and all features annotated as mitochondria or
477 chloroplast were removed from the table, and the abundance of bacterial taxa was
478 expressed as a percentage of the total 16S rRNA gene sequences. For alpha and beta
479 diversity, the feature table was rarefied to 10,434 reads. Shannon was used as an alpha

480 diversity index, and principal coordinates analysis (PCoA) based on weighted UniFrac
481 distances was used for beta diversity. The R package *qiime2R*
482 (https://github.com/jbisanz/qiime2R) was used for visualization.

483 **ITS sequencing and fungal community analysis**

484 The ITS1 region of the fungal DNA was amplified using the Phusion High-Fidelity DNA
485 polymerase (Thermo Scientific) with ITS1-F/ITS2 primer pair (ITS1-F: 5'-
486 CTTGGTCATTTAGAGGAAGTAA-3', ITS2: 5'-GCTGCGTTCTTCATCGATGC -3')[42,43],
487 which were conjugated with overhang adapter sequences for Illumina MiSeq. DNA library
488 construction and sequencing were conducted following the same procedures for 16S
489 rRNA gene sequencing.

490 The raw sequencing reads were processed using the QIIME2 pipeline [46]. The reads
491 were trimmed using Q2-ITSxpress [49]. Trimmed sequence reads were denoised, and
492 sequence variants were identified by DADA2 [47]. Taxonomy was assigned using a pre-
493 trained Naïve Bayes classifier on the UNITE v8.2 database [50]. Singletons were removed
494 from the table, and the abundance of fungal taxa was expressed as a percentage of total
495 sequence reads.

496 **RNA extraction from tissues**

497 Small pieces of the small intestine (ileum) and the kidney were stored in RNAlater
498 (Invitrogen). Total RNA from tissues was extracted using PureLink™ RNA Mini Kit
499 (Invitrogen) or RNeasy Plus Mini Kit (Qiagen) according to the manufacturer's protocol
500 and was stored at −20°C until further processing.

501 **Quantitative PCR (qPCR)**

502 cDNA was synthesized from isolated RNA with M-MLV Reverse Transcriptase
503 (Invitrogen). qPCR reactions were prepared using Maxima SYBR Green/ROX qPCR
504 Master Mix (Thermo Scientific) with primer set for *Il17a* (F:
505 ATCAGGACGCGCAAACATGA, R: TTGGACACGCTGAGCTTTGA) gene. Gene
506 expression was normalized to *Gapdh* (F: TGGCAAAGTGGAGATTGTTGCC, R:
507 AAGATGGTGATGGGCTTCCCG) and relative expression was calculated using the $^{\Delta\Delta}$Ct
508 method.

509 **RNA-Seq**

510 Extracted RNA samples were submitted for library construction and sequencing
511 (Novogene). The constructed libraries were sequenced on the Illumina NovaSeq X Plus
512 platform (Paired-end 150 bp). Adapter and low-quality reads were trimmed from the raw
513 sequence reads using Trimmomatic [51]. Trimmed sequence reads were aligned to the
514 mm10 mouse genome using the STAR aligner [52]. DESeq2 [53] was used to identify
515 differentially expressed genes (DEGs) between groups when $P < 0.05$. The heatmap and
516 volcano plot were drawn using the R packages Complex heatmap [54] and
517 EnhancedVolcano (https://github.com/kevinblighe/EnhancedVolcano), respectively. The
518 cell-specific gene list was obtained from PanglaoDB [55] and utilized as a cell marker gene
519 set for gene set enrichment analysis (GSEA). The R package clusterProfiler [56] was used
520 to perform GSEA.

521 **Fluorescence *in situ* hybridization (FISH)**

522 The small intestine and the colon were fixed in Methacarn (Bioworld) and embedded in
523 paraffin. Tissues were sectioned at 7 μm and deparaffinized in xylene followed by
524 rehydration in 95% EtOH, 90% EtOH, and H_2O. After deparaffinization and rehydration,

525 tissue sections were hybridized with universal bacterial probes (Alexa 488-
526 GCTGCCTCCCGTAGGAGT; Alexa 488-GCAGCCACCCGTAGGTGT) and a universal
527 fungal probe (Alexa 555-CTCTGGCTTCACCCTATTC) directed against the 16S rRNA
528 gene and 28S rRNA gene, respectively. DAPI was used to stain the nucleus.

529 **Intestinal cell staining**

530 The small intestine was fixed in Methacarn (Bioworld) and embedded in paraffin. Fixed
531 tissues were sectioned at 7 μm and deparaffinized in xylene followed by rehydration in
532 100% EtOH, 95% EtOH, 70% EtOH, and H_2O.

533 For tuft cells, slides were incubated in citrate buffer (10 mM Trisodium citrate, 0.05%
534 Tween 20, pH 6.0) for 20 min at 95 °C for antigen retrieval. Slides were blocked with 1%
535 bovine serum albumin (BSA) followed by overnight incubation with rabbit anti-mouse
536 DCAMKL1 (Abcam) antibodies at 4 °C. After incubation, slides were washed and
537 incubated with goat anti-rabbit Alexa Fluor 546 (Invitrogen) secondary antibodies for 1 h
538 at room temperature. Slides were counterstained with DAPI.

539 For goblet cells, slides were incubated with Alcian blue (StatLab) for 30 min, followed
540 by washing in running tap water for 2 min. Slides were counterstained with hematoxylin
541 for 2 min, followed by washing in running tap water for 30 sec. The slides were 10 dips in
542 the clarifier and bluing reagent with washing in tap water, respectively. Slides were
543 dehydrated in 95% EtOH, 100% EtOH, and xylene.

544 **Scanning electron microscopy (SEM) & transmission electron microscopy (TEM)**

545 For SEM, *K. pintolopesii* cultures were washed twice with sterile PBS, and a thin layer
546 was applied to the coverslips. The coverslips were fixed in fixation buffer (2.5%
547 glutaraldehyde, 0.15 M sodium cacodylate, 2% paraformaldehyde, 2 mM calcium chloride,

548 0.1 M sucrose, pH 7.4), followed by incubation for 2 h at room temperature. For the small
549 intestine, sections of the tissue were flushed with sterile PBS and then cut into 1 cm
550 sections. They were incubated in the same fixation buffer as previously described. After
551 incubation, the coverslips were washed three times with washing buffer (2 mM calcium
552 chloride, 0.15 M sodium cacodylate, 0.1 M sucrose). After washing, samples were
553 incubated overnight in 2% osmium tetroxide, 2.5% glutaraldehyde, 0.15 M sodium
554 cacodylate, and 2% paraformaldehyde. Samples were washed with DI water three times
555 and dehydrated in an EtOH gradient as follows: 20%, 50%, 70%, 90%, 95% and then
556 100%. Each EtOH step was incubated for 20 min at room temperature and then washed
557 twice with 100% EtOH. Samples were flash dehydrated using a critical point dryer and
558 then mounted on coverslips for imaging. Thermo Apreo SEM was used for imaging.

559 For TEM, *K. pintolopesii* cultures were pelleted in the 1.5 mL Eppendorf tubes. The
560 fixation buffer was added to the tubes and incubated for 2 h at room temperature. The
561 samples were then washed three times with the washing buffer. After washing, samples
562 were incubated overnight in 2% osmium tetroxide, 2.5% glutaraldehyde, 0.15 M sodium
563 cacodylate, and 2% paraformaldehyde. Samples were washed with DI water three times,
564 followed by incubation overnight at 4 °C in saturated uranyl acetate solution. The next
565 day, samples were dehydrated in the EtOH gradient as we described in SEM preparation
566 and washed three times in 100% EtOH. Then, the samples were infiltrated with Hard
567 Spurr's resin and rocked on a rotator at room temperature. The gradient started at 25%
568 Hard Spurr’s and 75% EtOH and gradually increased until 100% resin. Each step lasted
569 2 h, and the final 100% resin step was left overnight. The samples in resin were placed

570 in resin molds and then let to harden for 18-24 h at 60 °C. The pellets in resin were cut
571 with a knife into 100-200 nm sections and observed on PHILIPS 410 TEM.

572 ***Heligmosomoides polygyrus* infection**

573 *H. polygyrus* L3 larvae were orally gavaged to mice (200 L3 larvae per mouse). After
574 infection, fecal samples were collected every week. Fecal samples were resuspended in
575 water and mixed with the same volume of supersaturated salt solution. The resuspended
576 fecal solution was immediately loaded on a McMaster counting chamber (Eggzamin) and
577 eggs were counted under the microscope. The counted eggs were normalized by fecal
578 weight.

579 **Statistical analysis**

580 All statistical analysis and plotting were performed on R (https://www.R-project.org) and
581 Prism (GraphPad). The normality of data was assessed by the Shapiro-Wilk test. If data
582 followed normal distribution, parametric tests (unpaired two-tailed t-test for two groups,
583 One-way ANOVA with Tukey's multiple comparisons test for more than two groups) were
584 performed. If data did not follow normal distribution, non-parametric tests (Mann-Whitney
585 test for two groups, Kruskal-Wallis test with Dunn's multiple comparisons test for more
586 than two groups) were performed to find significant differences between groups. For the
587 survival curve, the log-rank (Mantel-Cox) test was used to find significant differences
588 between groups. A two-way ANOVA test was used to find significant differences in body
589 weight changes at each time point between the two groups. *$p < 0.05$, **$p < 0.01$, ***$p <$
590 0.001, ****$p<0.0001$.

591

592 **Data availability**

593 Raw sequence reads from 16S and ITS sequencing have been deposited in the NCBI
594 Sequence Read Archive (SRA) under accession number PRJNA1183864. Bulk RNA-seq
595 data have been deposited in the NCBI GEO database under accession number
596 GSE281418. This paper does not report the original code.
597

598 **Acknowledgments**

599 Schematics were created with BioRender.com. We thank Dr. Richard Bennett (Brown
600 University) for providing *S. cerevisiae* BY4717, *C. albicans* 529L, *C. albicans* SC5314,
601 *C. parapsilosis* ATCC22019, and *C. tropicalis* MYA-3404 strains. GH was supported by
602 an American Association of Immunologists Careers in Immunology Fellowship. NNJ is
603 supported by the Damon Runyon Cancer Research Foundation (DRG-2427-21) and
604 NIAID 1K22AI177360-01. SV is supported by R01DK113265, P20GM109035 (pilot
605 project) and Brown University Seed grant. LKB is supported by Searle Scholar
606 Foundation and this work is also supported by Brown University Seed grant. The Thermo
607 Apreo VS SEM was purchased with a high-end instrumentation grant from the Office of
608 the Director at the National Institutes of Health (S10OD023461).
609

610 **Author contributions**

611 Conceptualization: SV, LKB, GH; Methodology: SV, LKB, GH, RY, MHH, NNJ;
612 Investigation: SV, LKB, GH, RY, MHH, AB, KB, JP; Resources: SV, LKB, NNJ; Funding
613 acquisition: SV, LKB; Supervision: SV, LKB; Writing – original draft: SV, LKB, GH; Writing
614 – review & editing: SV, LKB, GH

Competing interests

The authors declare no competing interests.

620 **References**

621 1 Koropatnick, T. A. *et al.* Microbial factor-mediated development in a host-
622 bacterial mutualism. *Science* **306**, 1186-1188 (2004).
623 https://doi.org:10.1126/science.1102218
624 2 Pais, R., Lohs, C., Wu, Y., Wang, J. & Aksoy, S. The obligate mutualist
625 Wigglesworthia glossinidia influences reproduction, digestion, and immunity
626 processes of its host, the tsetse fly. *Appl Environ Microbiol* **74**, 5965-5974 (2008).
627 https://doi.org:10.1128/AEM.00741-08
628 3 Chung, H. *et al.* Gut immune maturation depends on colonization with a host-
629 specific microbiota. *Cell* **149**, 1578-1593 (2012).
630 https://doi.org:10.1016/j.cell.2012.04.037
631 4 Koh, A. Y. Murine models of Candida gastrointestinal colonization and
632 dissemination. *Eukaryot Cell* **12**, 1416-1422 (2013).
633 https://doi.org:10.1128/EC.00196-13
634 5 Koh, A. Y., Kohler, J. R., Coggshall, K. T., Van Rooijen, N. & Pier, G. B. Mucosal
635 damage and neutropenia are required for Candida albicans dissemination. *PLoS*
636 *Pathog* **4**, e35 (2008). https://doi.org:10.1371/journal.ppat.0040035
637 6 Kumamoto, C. A. Inflammation and gastrointestinal Candida colonization. *Curr*
638 *Opin Microbiol* **14**, 386-391 (2011). https://doi.org:10.1016/j.mib.2011.07.015
639 7 Yeung, F. *et al.* Altered Immunity of Laboratory Mice in the Natural Environment
640 Is Associated with Fungal Colonization. *Cell Host Microbe* **27**, 809-822 e806
641 (2020). https://doi.org:10.1016/j.chom.2020.02.015

642 8 Rosshart, S. P. *et al.* Laboratory mice born to wild mice have natural microbiota
643 and model human immune responses. *Science* **365** (2019).
644 https://doi.org:10.1126/science.aaw4361
645 9 Beura, L. K. *et al.* Normalizing the environment recapitulates adult human
646 immune traits in laboratory mice. *Nature* **532**, 512-516 (2016).
647 https://doi.org:10.1038/nature17655
648 10 Abolins, S. *et al.* The comparative immunology of wild and laboratory mice, Mus
649 musculus domesticus. *Nat Commun* **8**, 14811 (2017).
650 https://doi.org:10.1038/ncomms14811
651 11 Ma, J. *et al.* Laboratory mice with a wild microbiota generate strong allergic
652 immune responses. *Sci Immunol* **8**, eadf7702 (2023).
653 https://doi.org:10.1126/sciimmunol.adf7702
654 12 Chen, Y. H. *et al.* Rewilding of laboratory mice enhances granulopoiesis and
655 immunity through intestinal fungal colonization. *Sci Immunol* **8**, eadd6910 (2023).
656 https://doi.org:10.1126/sciimmunol.add6910
657 13 Sekeresova Kralova, J. *et al.* Competitive fungal commensalism mitigates
658 candidiasis pathology. *J Exp Med* **221** (2024).
659 https://doi.org:10.1084/jem.20231686
660 14 Liao, Y. *et al.* Fungal symbiont transmitted by free-living mice promotes type 2
661 immunity. *Nature* (2024). https://doi.org:10.1038/s41586-024-08213-2
662 15 Ivanov, II *et al.* Induction of intestinal Th17 cells by segmented filamentous
663 bacteria. *Cell* **139**, 485-498 (2009). https://doi.org:10.1016/j.cell.2009.09.033

664 16 Villarino, N. F. *et al.* Composition of the gut microbiota modulates the severity of
665 malaria. *Proc Natl Acad Sci U S A* **113**, 2235-2240 (2016).
666 https://doi.org:10.1073/pnas.1504887113
667 17 Hedin, K. A. *et al.* Effects of broad-spectrum antibiotics on the colonisation of
668 probiotic yeast Saccharomyces boulardii in the murine gastrointestinal tract. *Sci*
669 *Rep* **12**, 8862 (2022). https://doi.org:10.1038/s41598-022-12806-0
670 18 Jiang, T. T. *et al.* Commensal Fungi Recapitulate the Protective Benefits of
671 Intestinal Bacteria. *Cell Host Microbe* **22**, 809-816 e804 (2017).
672 https://doi.org:10.1016/j.chom.2017.10.013
673 19 Mellado, E. *et al.* Sustained gastrointestinal colonization and systemic
674 dissemination by Candida albicans, Candida tropicalis and Candida parapsilosis
675 in adult mice. *Diagn Microbiol Infect Dis* **38**, 21-28 (2000).
676 https://doi.org:10.1016/s0732-8893(00)00165-6
677 20 Ost, K. S. & Round, J. L. Commensal fungi in intestinal health and disease. *Nat*
678 *Rev Gastroenterol Hepatol* **20**, 723-734 (2023). https://doi.org:10.1038/s41575-
679 023-00816-w
680 21 Roberts, K. *et al.* Candida tropicalis Affects Candida albicans Virulence by
681 Limiting Its Capacity to Adhere to the Host Intestinal Surface, Leading to
682 Decreased Susceptibility to Colitis in Mice. *J Fungi (Basel)* **10** (2024).
683 https://doi.org:10.3390/jof10040245
684 22 Doan, H. T. *et al.* Candida tropicalis-derived vitamin B3 exerts protective effects
685 against intestinal inflammation by promoting IL-17A/IL-22-dependent epithelial

686 barrier function. *Gut Microbes* **16**, 2416922 (2024).
687 https://doi.org:10.1080/19490976.2024.2416922
688 23 Rahman, D., Mistry, M., Thavaraj, S., Challacombe, S. J. & Naglik, J. R. Murine
689 model of concurrent oral and vaginal Candida albicans colonization to study
690 epithelial host-pathogen interactions. *Microbes Infect* **9**, 615-622 (2007).
691 https://doi.org:10.1016/j.micinf.2007.01.012
692 24 McDonough, L. D. *et al.* Candida albicans Isolates 529L and CHN1 Exhibit
693 Stable Colonization of the Murine Gastrointestinal Tract. *mBio* **12**, e0287821
694 (2021). https://doi.org:10.1128/mBio.02878-21
695 25 Bacher, P. *et al.* Human Anti-fungal Th17 Immunity and Pathology Rely on
696 Cross-Reactivity against Candida albicans. *Cell* **176**, 1340-1355 e1315 (2019).
697 https://doi.org:10.1016/j.cell.2019.01.041
698 26 Shao, T. Y. *et al.* Commensal Candida albicans Positively Calibrates Systemic
699 Th17 Immunological Responses. *Cell Host Microbe* **25**, 404-417 e406 (2019).
700 https://doi.org:10.1016/j.chom.2019.02.004
701 27 Leonardi, I. *et al.* Mucosal fungi promote gut barrier function and social behavior
702 via Type 17 immunity. *Cell* **185**, 831-846 e814 (2022).
703 https://doi.org:10.1016/j.cell.2022.01.017
704 28 Gerbe, F. *et al.* Intestinal epithelial tuft cells initiate type 2 mucosal immunity to
705 helminth parasites. *Nature* **529**, 226-230 (2016).
706 https://doi.org:10.1038/nature16527

29 Howitt, M. R. *et al.* Tuft cells, taste-chemosensory cells, orchestrate parasite type 2 immunity in the gut. *Science* **351**, 1329-1333 (2016). https://doi.org:10.1126/science.aaf1648

30 Sasaki, S., Ishida, Y., Nishio, N., Ito, S. & Isobe, K. Thymic involution correlates with severe ulcerative colitis induced by oral administration of dextran sulphate sodium in C57BL/6 mice but not in BALB/c mice. *Inflammation* **31**, 319-328 (2008). https://doi.org:10.1007/s10753-008-9081-3

31 Tsuchiya, T. *et al.* Role of gamma delta T cells in the inflammatory response of experimental colitis mice. *J Immunol* **171**, 5507-5513 (2003). https://doi.org:10.4049/jimmunol.171.10.5507

32 Rosshart, S. P. *et al.* Wild Mouse Gut Microbiota Promotes Host Fitness and Improves Disease Resistance. *Cell* **171**, 1015-1028 e1013 (2017). https://doi.org:10.1016/j.cell.2017.09.016

33 Huggins, M. A. *et al.* Microbial Exposure Enhances Immunity to Pathogens Recognized by TLR2 but Increases Susceptibility to Cytokine Storm through TLR4 Sensitization. *Cell Rep* **28**, 1729-1743 e1725 (2019). https://doi.org:10.1016/j.celrep.2019.07.028

34 Netea, M. G., Joosten, L. A., van der Meer, J. W., Kullberg, B. J. & van de Veerdonk, F. L. Immune defence against Candida fungal infections. *Nat Rev Immunol* **15**, 630-642 (2015). https://doi.org:10.1038/nri3897

35 Underhill, D. M. & Iliev, I. D. The mycobiota: interactions between commensal fungi and the host immune system. *Nat Rev Immunol* **14**, 405-416 (2014). https://doi.org:10.1038/nri3684

730 36 Han, G., Luong, H. & Vaishnava, S. Low abundance members of the gut
731 microbiome exhibit high immunogenicity. *Gut Microbes* **14**, 2104086 (2022).
732 https://doi.org:10.1080/19490976.2022.2104086
733 37 Oh, J. H. *et al.* Naturalized immune responses are stable over years in a colony
734 of laboratory mice with wild-derived microbiota. *Immunity* **58**, 2305-2319 e2305
735 (2025). https://doi.org:10.1016/j.immuni.2025.07.004
736 38 Runge, S. *et al.* Laboratory mice engrafted with natural gut microbiota possess a
737 wildling-like phenotype. *Nat Commun* **16**, 5301 (2025).
738 https://doi.org:10.1038/s41467-025-60554-2
739 39 Roble, G. S., Gillespie, V. & Lipman, N. S. Infectious disease survey of Mus
740 musculus from pet stores in New York City. *J Am Assoc Lab Anim Sci* **51**, 37-41
741 (2012).
742 40 Parker, S. E., Malone, S., Bunte, R. M. & Smith, A. L. Infectious diseases in wild
743 mice (Mus musculus) collected on and around the University of Pennsylvania
744 (Philadelphia) Campus. *Comp Med* **59**, 424-430 (2009).
745 41 Dammann, P. *et al.* Infectious microorganisms in mice (Mus musculus)
746 purchased from commercial pet shops in Germany. *Lab Anim* **45**, 271-275
747 (2011). https://doi.org:10.1258/la.2011.010183
748 42 Gardes, M. & Bruns, T. D. ITS primers with enhanced specificity for
749 basidiomycetes--application to the identification of mycorrhizae and rusts. *Mol*
750 *Ecol* **2**, 113-118 (1993). https://doi.org:10.1111/j.1365-294x.1993.tb00005.x

751 43 White, T. J., Bruns, T., Lee, S. & Taylor, J. in *PCR Protocols: A Guide to*
752 *Methods and Applications* (eds M. A. Innis, D. H. Gelfand, J. J. Sninsky, & T. J.
753 White) 315-322 (Academic Press, 1990).
754 44 Beura, L. K. *et al.* Lymphocytic choriomeningitis virus persistence promotes
755 effector-like memory differentiation and enhances mucosal T cell distribution. *J*
756 *Leukoc Biol* **97**, 217-225 (2015). https://doi.org:10.1189/jlb.1HI0314-154R
757 45 Grizotte-Lake, M. *et al.* Commensals Suppress Intestinal Epithelial Cell Retinoic
758 Acid Synthesis to Regulate Interleukin-22 Activity and Prevent Microbial
759 Dysbiosis. *Immunity* **49**, 1103-1115 e1106 (2018).
760 https://doi.org:10.1016/j.immuni.2018.11.018
761 46 Bolyen, E. *et al.* Reproducible, interactive, scalable and extensible microbiome
762 data science using QIIME 2. *Nat Biotechnol* **37**, 852-857 (2019).
763 https://doi.org:10.1038/s41587-019-0209-9
764 47 Callahan, B. J. *et al.* DADA2: High-resolution sample inference from Illumina
765 amplicon data. *Nat Methods* **13**, 581-583 (2016).
766 https://doi.org:10.1038/nmeth.3869
767 48 Yilmaz, P. *et al.* The SILVA and "All-species Living Tree Project (LTP)"
768 taxonomic frameworks. *Nucleic Acids Res* **42**, D643-648 (2014).
769 https://doi.org:10.1093/nar/gkt1209
770 49 Rivers, A. R., Weber, K. C., Gardner, T. G., Liu, S. & Armstrong, S. D. ITSxpress:
771 Software to rapidly trim internally transcribed spacer sequences with quality
772 scores for marker gene analysis. *F1000Res* **7**, 1418 (2018).
773 https://doi.org:10.12688/f1000research.15704.1

774 50 Nilsson, R. H. *et al.* The UNITE database for molecular identification of fungi:
775 handling dark taxa and parallel taxonomic classifications. *Nucleic Acids Res* **47**,
776 D259-D264 (2019). https://doi.org:10.1093/nar/gky1022
777 51 Bolger, A. M., Lohse, M. & Usadel, B. Trimmomatic: a flexible trimmer for Illumina
778 sequence data. *Bioinformatics* **30**, 2114-2120 (2014).
779 https://doi.org:10.1093/bioinformatics/btu170
780 52 Dobin, A. *et al.* STAR: ultrafast universal RNA-seq aligner. *Bioinformatics* **29**, 15-
781 21 (2013). https://doi.org:10.1093/bioinformatics/bts635
782 53 Love, M. I., Huber, W. & Anders, S. Moderated estimation of fold change and
783 dispersion for RNA-seq data with DESeq2. *Genome Biol* **15**, 550 (2014).
784 https://doi.org:10.1186/s13059-014-0550-8
785 54 Gu, Z. Complex heatmap visualization. *Imeta* **1**, e43 (2022).
786 https://doi.org:10.1002/imt2.43
787 55 Franzen, O., Gan, L. M. & Bjorkegren, J. L. M. PanglaoDB: a web server for
788 exploration of mouse and human single-cell RNA sequencing data. *Database*
789 *(Oxford)* **2019** (2019). https://doi.org:10.1093/database/baz046
790 56 Xu, S. *et al.* Using clusterProfiler to characterize multiomics data. *Nat Protoc* **19**,
791 3292-3320 (2024). https://doi.org:10.1038/s41596-024-01020-z

792

793

794

795

Figures

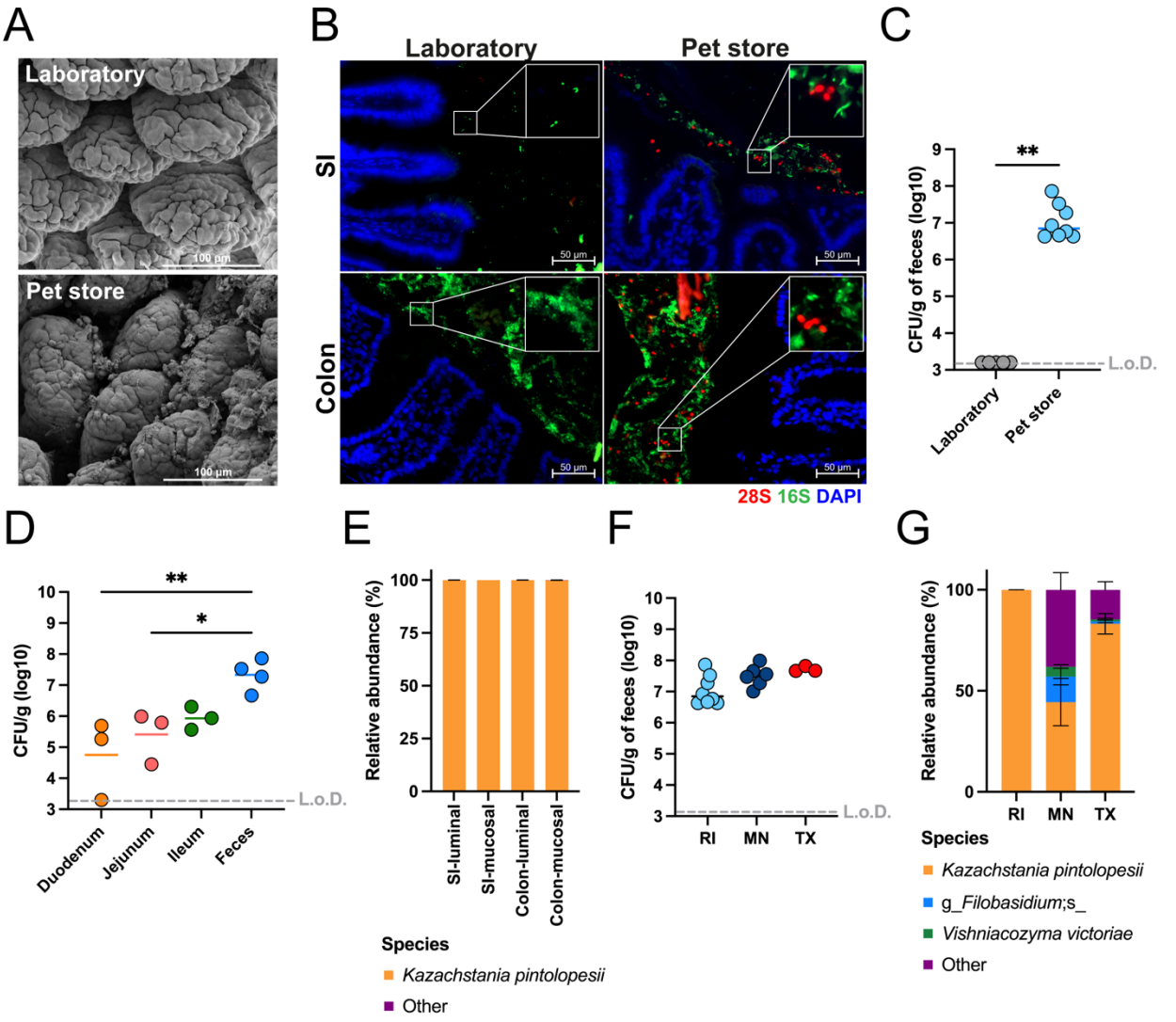

Fig. 1. *K. pintolopesii* is the dominant fungus in the gut of pet store mice. (A) Representative scanning electron microscopy (SEM) image of the small intestine of laboratory mice and pet store mice. (B) Representative fluorescence *in situ* hybridization (FISH) images of fungal colonization in the small intestine and the colon of laboratory mice and pet store mice. Tissues were stained with DAPI (nuclei; blue), EUB338 probe (bacteria; green), and 28S probe (fungi; red). (C) Fungal burden in the feces of laboratory mice (n = 5) and pet store mice (n = 8). (D) Fungal burden in the intestinal tract of the pet

store mice (*n* = 3 for tissues and *n* = 4 for feces). (E) Bar plot of relative abundance of fungal species from the ITS-marker gene sequencing at different sections of the intestine – luminal and mucosal part of the small intestine and the colon (*n* = 4 for SI-mucosal and *n* = 5 for other samples). Fungal burden (F) (RI, *n* = 8; MN, *n* = 6; TX, *n* =3) and bar plot of relative abundance of fungal species (G) in the feces of pet store mice (RI, *n* = 5; MN, *n* = 6; TX, *n* =8) in Rhode Island (RI), Minnesota (MI), and Texas (TX) in the USA. Bars indicate mean ± SEM. *$p < 0.05$ and **$p < 0.01$. L.o.D., limit of detection.

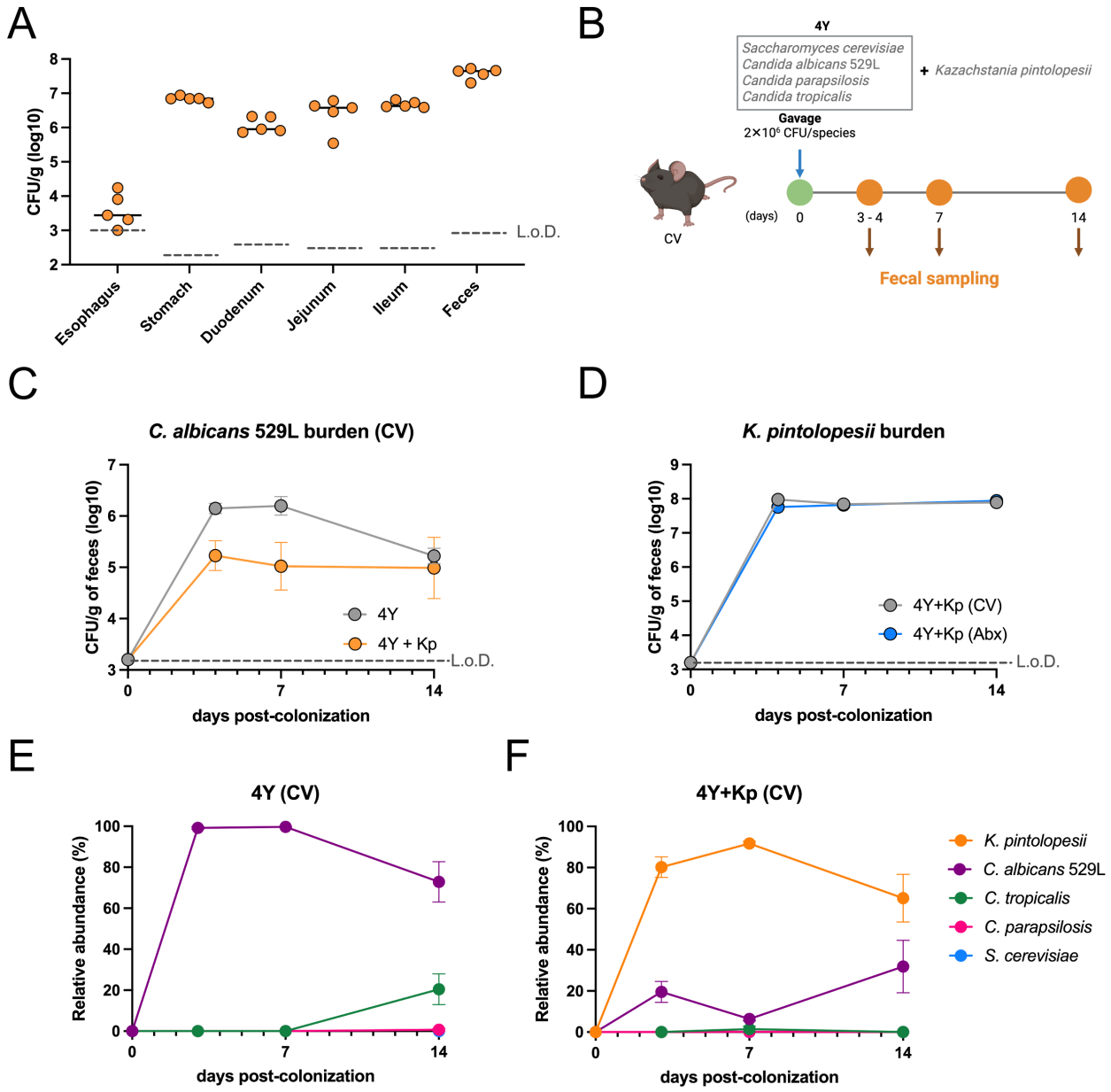

Fig. 2. *K. pintolopesii* stably colonizes laboratory mice and provides colonization resistance against non-murine fungi. (A) Fungal burden in the gastrointestinal tract of mice at 14 days post-colonization of *K. pintolopesii* (n = 5). (B) Scheme of fungal competition assay in the conventional mice. (C) Burden of the *C. albicans* 529L in conventional mice with (4Y + Kp) or without *K. pintolopesii* (4Y). (D) Burden of the *K. pintolopesii* in conventional and antibiotic-treated mice. Line plot of relative abundance of

820 fungal species from ITS-marker gene sequencing of the feces at different time points
821 (days 3, 7, and 14) in conventional mice without (E) or with *K. pintolopesii* (F) (*n* = 5 per
822 group). Dots indicate mean ± SEM. L.o.D., limit of detection. CV, conventional mice. Abx,
823 antibiotic-treated mice. 4Y, four different yeast strains. Kp, *K. pintolopesii*-colonized mice.

824

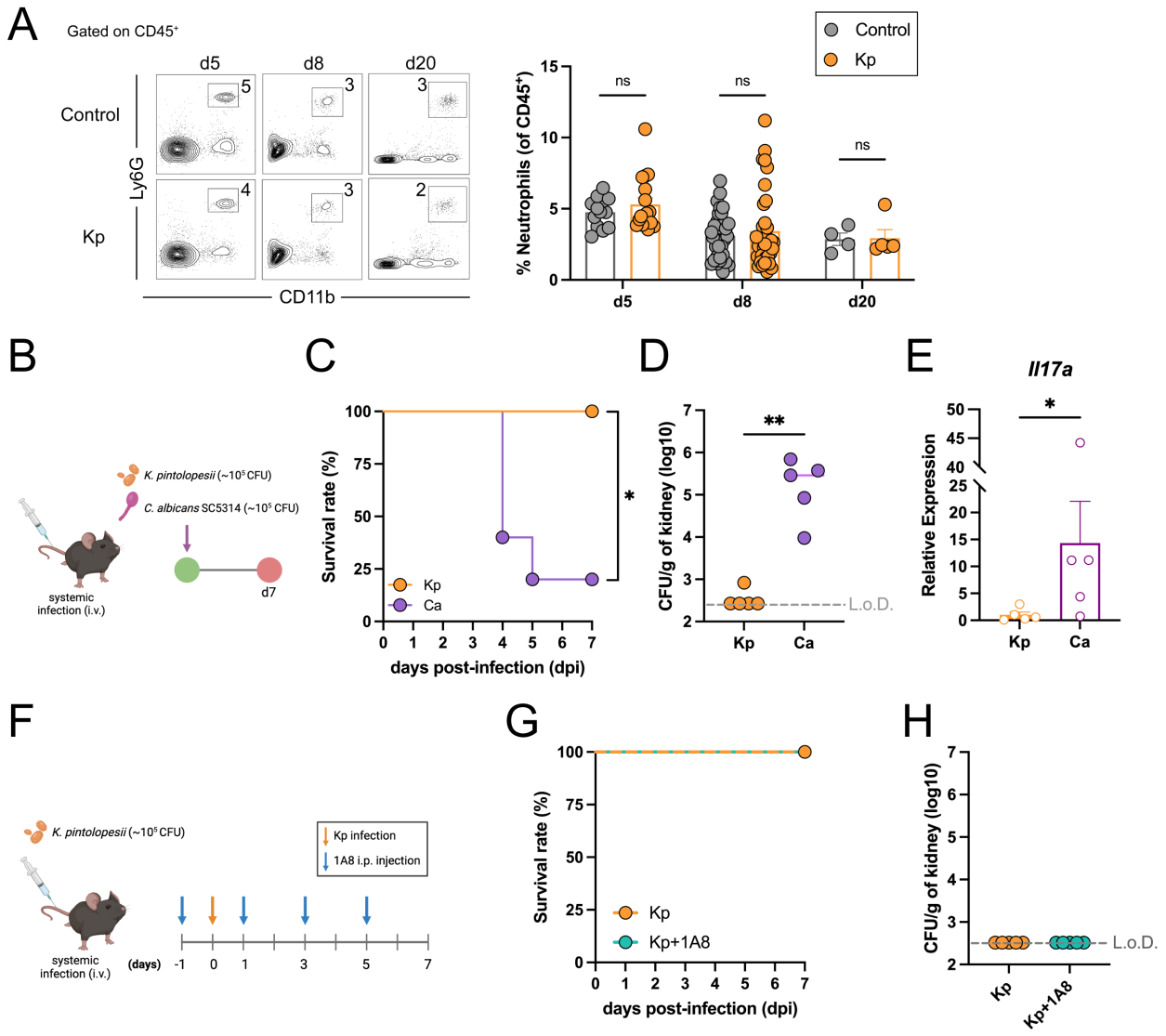

825

826 **Fig. 3. The systemic challenge with *K. pintolopesii* is efficiently resolved in a**
827 **neutrophil-independent manner.** (A) Representative flow cytometry plots and
828 frequency of circulating neutrophils in the peripheral blood at 5 (Control, *n* = 13; Kp, *n* =
829 17), 8 (Control, *n* = 30; Kp, *n* = 35), and 20 days (Control, *n* = 4; Kp, *n* = 5) post-
830 colonization of *K. pintolopesii*. Neutrophil populations were gated as $CD45^+$ $B220^-$
831 $CD11b^+$ $Ly6G^+$. (B) Scheme of the systemic challenge with *K. pintolopesii* or *C. albicans*
832 (*n* = 5 per group). (C) The survival curve after *K. pintolopesii* or *C. albicans* systemic

833 infection. Fungal burden (D) and *Il17a* gene expression (E) in the kidney after *C. albicans*
834 or *K. pintolopesii* infection. (F) Experimental schedule of neutrophil depletion and *K.*
835 *pintolopesii* infection (*n* = 5 per group). (G) The survival curve after *K. pintolopesii*
836 systemic infection with or without neutrophil depletion. (H) Fungal burden in the kidney
837 after *K. pintolopesii* systemic infection with or without neutrophil depletion. Bars indicate
838 mean ± SEM. *$p < 0.05$ and **$p < 0.01$. L.o.D., limit of detection. Kp, *K. pintolopesii*-
839 colonized mice. Ca, *C. albicans*-colonized mice.

840

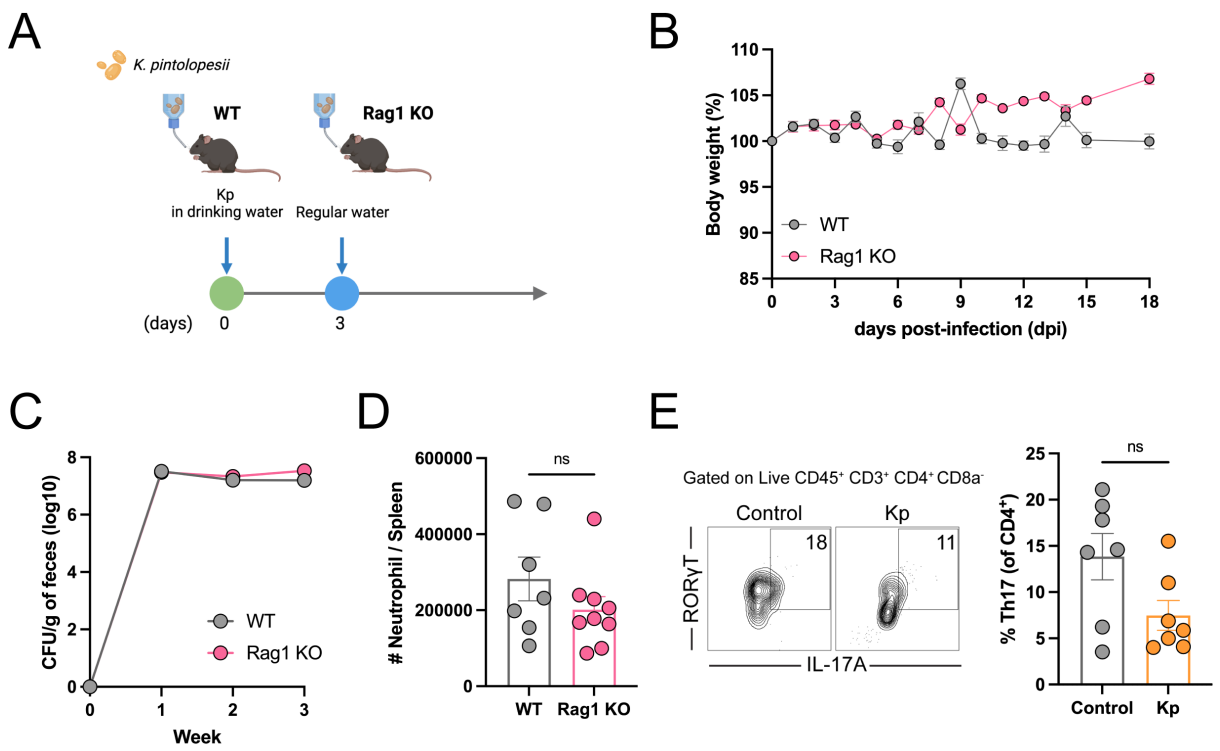

Fig. 4. *K. pintolopesii* colonizes the intestine of mice in an adaptive immunity-independent manner. (A) Scheme of the *K. pintolopesii* colonization in wild-type (WT, *n* = 13) and adaptive immunity-deficient Rag1 knock-out mice (Rag1 KO, *n* = 18). (B) Body weight changes of WT and Rag1 KO mice after *K. pintolopesii* colonization. (C) Fungal burden in the feces of WT and Rag1 KO mice. (D) The number of neutrophils in the spleen at 19 days post-colonization of *K. pintolopesii* (WT, *n* = 7; Rag1 KO, *n* = 9). (E) Representative flow cytometry plots and frequency of Th17 cells in the small intestinal lamina propria at 14 days (*n* = 7 per group) post-colonization of *K. pintolopesii*. Th17 populations were gated as live $CD45^+$ $CD3^+$ $CD4^+$ $CD8a^-$ IL-$17A^+$ $ROR\gamma T^+$. Bars indicate mean ± SEM. Kp, *K. pintolopesii*-colonized mice.

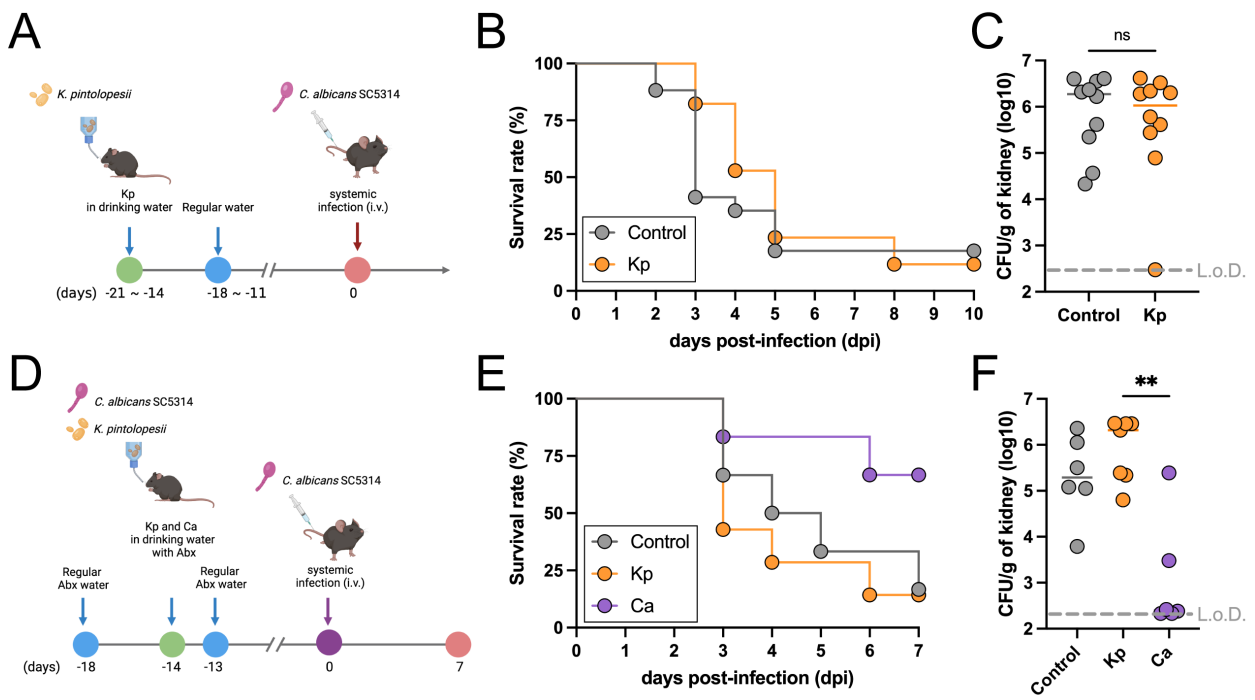

Fig. 5. Intestinal colonization of *K. pintolopesii* does not protect the host against systemic *C. albicans* challenge. (A) Scheme of the *C. albicans* systemic challenge in the *K. pintolopesii*-colonized mice. Survival rate (B) (n = 17 per group) and fungal burden in the kidney (C) (n = 10 per group) after *C. albicans* challenge in control and *K. pintolopesii*-colonized mice. (D) Scheme of the *C. albicans* systemic challenge in the *K. pintolopesii*- or *C. albicans*-colonized mice with antibiotics (Abx) treatment. Survival rate (E) and fungal burden in the kidney (F) after *C. albicans* challenge in control (n = 6), *K. pintolopesii*-colonized (n = 7), and *C. albicans*-colonized mice (n = 6). Kp, *K. pintolopesii*-colonized mice. Ca, *C. albicans*-colonized mice.

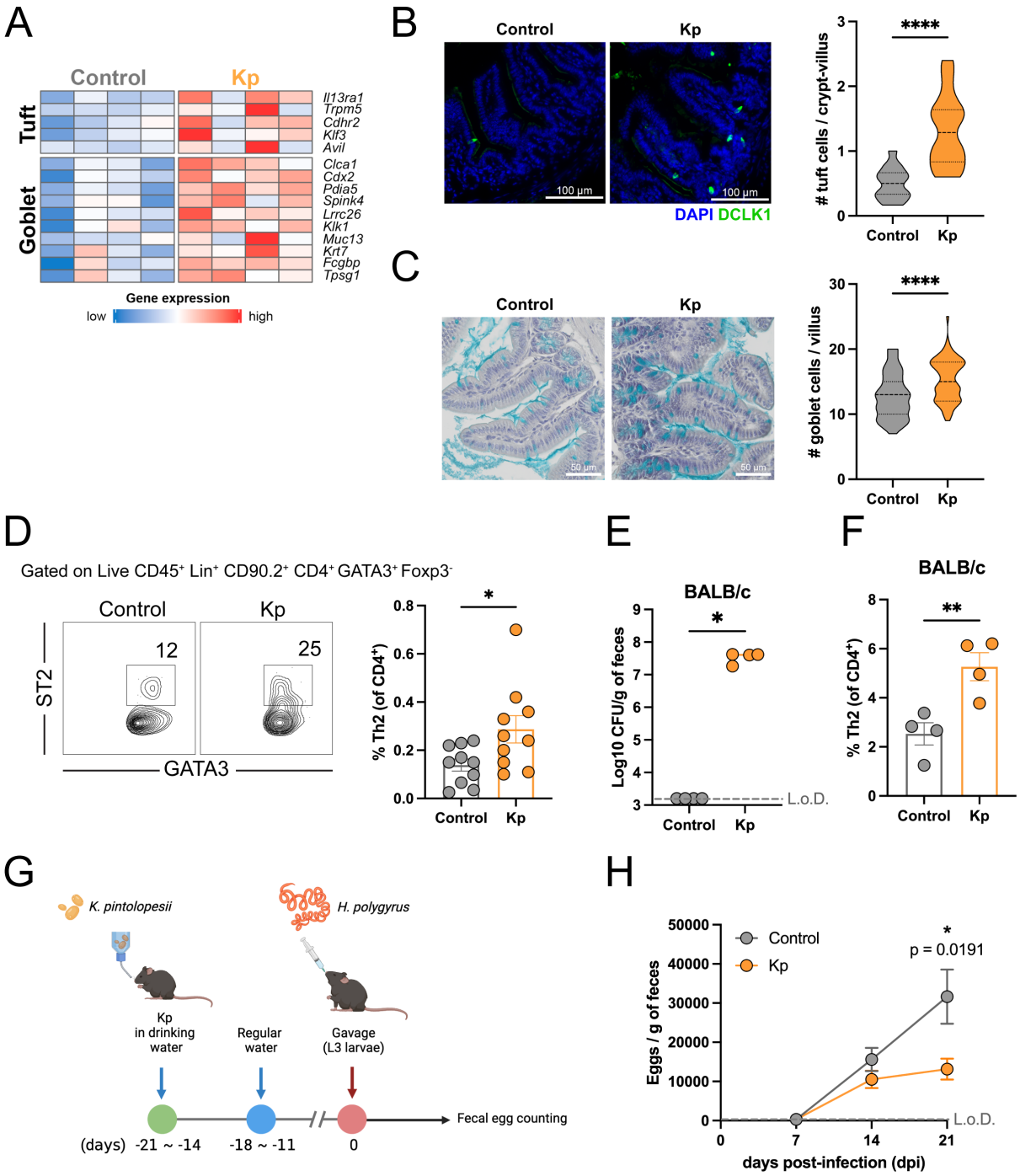

Fig. 6. *K. pintolopesii* colonization increases the tuft cell population and induces type 2 immune responses in the gut and protects the host against *H. polygyrus* infection. (A) The heat map of expression of the tuft cell and the goblet cell marker genes in the small intestine (n = 4 per group). (B) Representative image and the number of tuft

871 cells in the small intestine of control and *K. pintolopesii*-colonized mice. Tissues were
872 stained with DAPI (nuclei; blue) and DCLK1 (tuft cells; green). 1-7 images were used for
873 tuft cell counting per mouse, with 4–6 mice per group. (C) Representative image and the
874 number of goblet cells in the small intestine of control and *K. pintolopesii*-colonized mice.
875 Tissues were stained with hematoxylin (nuclei) and alcian blue (goblet cells). 6-15 villi
876 were chosen for goblet cell counting per mouse, with 4–5 mice per group. (D)
877 Representative flow cytometry plots and frequency of Th2 in the small intestinal lamina
878 propria of control and *K. pintolopesii*-colonized mice (n = 10 per group). Th2 populations
879 were gated as live $CD45^+$ Lin^+ $CD90.2^+$ $CD4^+$ $GATA3^+$ $Foxp3^-$ $ST2^+$. Lin: CD3ε, CD11b,
880 Ly-6G/Ly-6C, CD19. (E) Fungal burden in the feces of BALB/c mice after *K. pintolopesii*
881 colonization (n = 4 per group). (F) Frequency of Th2 in the small intestinal lamina propria
882 of control and *K. pintolopesii*-colonized BALB/c mice (n = 4 per group). (G) Scheme of
883 the *H. polygyrus* challenge. (H) The quantification of worm eggs in the feces of the control
884 and *K. pintolopesii*-colonized mice (Control, n = 9; Kp, n = 10). Bars indicate mean ± SEM.
885 *$p < 0.05$, **$p < 0.01$, and ****$p < 0.0001$. Kp, *K. pintolopesii*-colonized mice.

886